

# Temperature dependence of the hydrated electron's excited-state relaxation. I. Simulation predictions of resonance Raman and pump-probe transient absorption spectra of cavity and non-cavity models

Chen-Chen Zho,<sup>1</sup> Erik P. Farr,<sup>1</sup> William J. Glover,<sup>1,2,3,a)</sup> and Benjamin J. Schwartz<sup>1,b)</sup>

<sup>1</sup>Department of Chemistry and Biochemistry, University of California, Los Angeles, Los Angeles, California, 90095-1569, USA

<sup>2</sup>NYU-ECNU Center for Computational Chemistry at NYU Shanghai, Shanghai 200062, China

<sup>3</sup>NYU Shanghai, 1555 Century Avenue, Shanghai 200135, China

(Received 31 May 2017; accepted 31 July 2017; published online 18 August 2017)

We use one-electron non-adiabatic mixed quantum/classical simulations to explore the temperature dependence of both the ground-state structure and the excited-state relaxation dynamics of the hydrated electron. We compare the results for both the traditional cavity picture and a more recent non-cavity model of the hydrated electron and make definite predictions for distinguishing between the different possible structural models in future experiments. We find that the traditional cavity model shows no temperature-dependent change in structure at constant density, leading to a predicted resonance Raman spectrum that is essentially temperature-independent. In contrast, the non-cavity model predicts a blue-shift in the hydrated electron's resonance Raman O–H stretch with increasing temperature. The lack of a temperature-dependent ground-state structural change of the cavity model also leads to a prediction of little change with temperature of both the excited-state lifetime and hot ground-state cooling time of the hydrated electron following photoexcitation. This is in sharp contrast to the predictions of the non-cavity model, where both the excited-state lifetime and hot ground-state cooling time are expected to decrease significantly with increasing temperature. These simulation-based predictions should be directly testable by the results of future time-resolved photoelectron spectroscopy experiments. Finally, the temperature-dependent differences in predicted excited-state lifetime and hot ground-state cooling time of the two models also lead to different predicted pump-probe transient absorption spectroscopy of the hydrated electron as a function of temperature. We perform such experiments and describe them in Paper II [E. P. Farr *et al.*, *J. Chem. Phys.* **147**, 074504 (2017)], and find changes in the excited-state lifetime and hot ground-state cooling time with temperature that match well with the predictions of the non-cavity model. In particular, the experiments reveal stimulated emission from the excited state with an amplitude and lifetime that decreases with increasing temperature, a result in contrast to the lack of stimulated emission predicted by the cavity model but in good agreement with the non-cavity model. Overall, until *ab initio* calculations describing the non-adiabatic excited-state dynamics of an excess electron with hundreds of water molecules at a variety of temperatures become computationally feasible, the simulations presented here provide a definitive route for connecting the predictions of cavity and non-cavity models of the hydrated electron with future experiments. *Published by AIP Publishing.* [<http://dx.doi.org/10.1063/1.4985905>]

## I. INTRODUCTION

What happens when an excess electron, one more than what is needed for electrical neutrality, is released into a liquid? The resulting species is termed a solvated electron, and the nature of solvated electrons has been of intense interest as these objects serve as reaction intermediates in charge transfer and radiolysis reactions as well as provide a testbed for our understanding of quantum chemistry in dynamic disordered environments. Excess electrons in water, or hydrated electrons,<sup>1,2</sup> have been of particular interest to both experimentalists<sup>3–12</sup> and theorists.<sup>13–18</sup>

Despite this intense interest, questions still remain concerning the structure of the hydrated electron. The conventional picture has been that the hydrated electron carves out a cavity, locally expelling the water and behaving roughly as a particle in a quasi-spherical box.<sup>13,19–21</sup> Recently, however, both we<sup>14,22,23</sup> and others<sup>17,18</sup> have challenged this picture based on calculations that suggest that the excess electron's wavefunction encompasses several water molecules in a structure with only a small or even no central cavity. We note that our one-electron non-cavity pseudopotential has been criticized,<sup>24–26</sup> both for overbinding the electron energetically<sup>15,27</sup> and for predicting a negative molar solvation volume<sup>28</sup> when experiment suggests that this parameter should be positive.<sup>29</sup> Nevertheless, non-cavity hydrated electron models have been shown to account for

<sup>a)</sup>Electronic mail: [william.glover@nyu.edu](mailto:william.glover@nyu.edu)

<sup>b)</sup>Electronic mail: [schwartz@chem.ucla.edu](mailto:schwartz@chem.ucla.edu)

various experimental observations that the traditional cavity picture cannot explain, including the hydrated electron's resonance Raman spectral line shape,<sup>22,23</sup> behavior at the air/water interface,<sup>28</sup> and time-resolved photoelectron spectroscopy.<sup>30</sup>

Another important feature of hydrated electrons is that their properties are temperature dependent. It is well known that the absorption spectrum of the hydrated electron red-shifts with increasing temperature.<sup>8,31,32</sup> Although some of this red-shift results from the fact that the density of water decreases with increasing temperature at constant pressure,<sup>33</sup> careful experiments have shown conclusively that the absorption maximum of the hydrated electron's spectrum red-shifts by 2.2 meV/K with increasing temperature at constant water density.<sup>11,34</sup> Cavity models of the hydrated electron have failed to reproduce this constant-density temperature dependence, showing little to no temperature dependence.<sup>22,33,35,36</sup> Our non-cavity model, on the other hand, shows the correct qualitative trend with temperature, although the calculated absorption spectrum shift is about double that observed experimentally.<sup>22,23</sup>

What is it about cavity and non-cavity hydrated electron models that lead to such different predicted dependence on temperature? Most hydrated electron models are based on mixed quantum/classical (MQC) molecular dynamics (MD) simulations, where the water molecules are treated classically and only the excess electron is treated quantum mechanically, with the classical and quantum degrees of freedom coupled via a pseudopotential. (Of the few calculations based on density functional theory (DFT) with quantum mechanically treated water,<sup>17,18</sup> none as of yet have explored the temperature dependence of the calculated hydrated electron's properties, including those that have applied DFT *ex post facto* to configurations generated from MQC MD simulations.<sup>27,37,38</sup>) The pseudopotentials typically used in cavity models tend to be highly repulsive to account for Pauli exclusion interactions between the excess electron and the electrons in the occupied water molecular orbitals. We have recently argued, however, that correlation/dispersion interactions can lead to substantial attractions between an excess electron and water at short range and that proper inclusion of such interactions in a cavity-forming pseudopotential promotes non-cavity hydrated electron behavior.<sup>36</sup> Indeed, the pseudopotential we developed when originally proposing a non-cavity picture for the hydrated electron happens to do a good job of accounting for such interactions, even though this was not intentionally part of our original design.<sup>14</sup> It is largely the way the balance between these attractive and repulsive interactions (the former of which are missing in cavity models) changes with temperature that explains the hydrated electron's  $T$ -dependent spectral shift.<sup>22,23</sup>

In this work, we extend our understanding of the differences between cavity and non-cavity models by examining their predictions for the temperature dependence of the hydrated electron's excited-state dynamics. There has been relatively little experimental work<sup>8</sup> and no theoretical work that we are aware of examining the  $T$ -dependent behavior of the photoexcited hydrated electron, so this opens an entirely new avenue for predictions that can make direct contact with

experiment. We choose to focus on MQC MD simulations because at the present time, we are not aware of any *ab initio* methods that are capable of simulating hydrated electron excited-state dynamics with the requisite number of water molecules. We find that non-cavity hydrated electrons show a pronounced temperature dependence to their excited-state lifetime, a result of the fact that the solvation structure of the ground-state electron changes significantly with temperature. In contrast, cavity hydrated electrons show essentially no predicted change in excited-state lifetime, the result of a ground-state solvation structure that is constant with temperature. The different ground-state structures lead to different predicted temperature dependences for resonance Raman spectroscopy, and the different excited-state dynamics lead to different predicted temperature-dependent transient absorption and time-resolved photoelectron spectra.

In Paper II,<sup>39</sup> we perform temperature-dependent transient absorption measurements and find results that are in qualitative disagreement with the traditional cavity picture, but in excellent agreement with our non-cavity model. This reinforces the notion that a picture of the hydrated electron as a strongly repulsive, hydrophobic object that resides in a cavity is not consistent with its known temperature-dependent properties; hopefully temperature-dependent resonance Raman and time-resolved photoelectron spectroscopy experiments will be performed in the near future to further test the differing predictions of cavity and non-cavity hydrated electron models.

## II. COMPUTATIONAL METHODS

The equilibrium ground-state MQC MD simulations in this work were performed in the canonical (NVT) ensemble using in-house developed codes; the methods are essentially the same as those detailed in our previous published work on this topic.<sup>14,22,23,40,41</sup> Briefly, 499 water molecules were included in a cubic simulation box of length 24.64 Å with one excess electron. The excess electron was treated quantum mechanically, the wave function of which computed using a plane-wave basis set, while the water molecules were treated classically by the flexible simple point charge (SPC-flex)<sup>42</sup> model. The coordinates of the water molecules were propagated by the velocity Verlet algorithm. The simulations used periodic boundary conditions, and the temperature was enforced with a thermostat.<sup>43</sup> The quantum force exerted on the classical solvent molecules by the excess electron was calculated via the Hellmann-Feynman theorem.

For both the cavity and non-cavity models, the pseudopotentials we employed to account for the electron-water interactions were derived via the Phillips-Kleinman formalism.<sup>44-46</sup> In particular, we follow our previous work and use the pseudopotential developed by Turi and Borgis<sup>13</sup> (denoted as TB, below) as a representative cavity model for the hydrated electron, and our more recent pseudopotential<sup>14</sup> (referred to as LGS in literature) as a non-cavity hydrated electron. When solving Schrodinger's equation, we used a  $16^3$  or  $32^3$  plane wave basis for calculating the wave function of the TB and LGS hydrated electrons, respectively,

as needed to reach energy convergence. Our simulations employed minimum-image periodic boundary conditions, and all interactions were smoothly tapered to zero at 16 Å over a 2 Å range with a group-based cutoff.<sup>47</sup> We note that explicit treatment of the long-range interactions in MQC simulations does yield different results for the hydrated electron.<sup>15</sup> We have chosen to taper the interactions for the simulations discussed here, however, both because Ewald summation is known to give a stronger finite size effect for this system, as we have discussed in Ref. 28, and because this choice is consistent with our previously published work,<sup>14,22,23,41</sup> allowing for direct comparison to the data presented below.

For each hydrated electron model at each equilibrium temperature, we started by running a 200-ps adiabatic equilibrium trajectory along the electronic ground state. We then simulated the dynamics following photoexcitation from the ground state by picking 50 uncorrelated ground-state electron configurations and promoting the electron to one of the adiabatic excited states to create a microcanonical ensemble of non-equilibrium trajectories that each had a duration of  $\geq 1.5$  ps. A few individual sample trajectories are given in the [supplementary material](#). We chose the pump wavelength at the different equilibrium temperatures (1.22–1.76 eV for LGS, 1.70–1.75 eV for TB) such that the majority of the electrons were promoted to the lowest excited state. The larger range for pump wavelengths for the LGS model accounts for the fact that the equilibrium energy gap changes significantly with temperature whereas that for the TB model does not.<sup>22</sup>

The breakdown of the Born-Oppenheimer approximation (nonadiabatic dynamics) on the excited-state manifold was accounted for using Tully's fewest switches surface hopping (FSSH) algorithm.<sup>48</sup> We note that previous work has used a formalism based on Fermi's Golden Rule (FGR) to estimate the lifetime of hydrated electrons/water anion clusters.<sup>49</sup> The FGR formalism, however, relies on linear response, which unfortunately does not hold for photoexcitation of the hydrated electron.<sup>50</sup> This is why we have elected to simulate the non-adiabatic relaxation using the FSSH algorithm. It is important to note, however, that the FSSH algorithm does not provide a realistic picture of the decoherence that induces surface hopping for strongly coupled systems such as the hydrated electron.<sup>40</sup> This means that the excited-state lifetimes calculated in our non-equilibrium trajectories will at best be estimates of the true lifetime and that caution is recommended before attempting any type of direct comparison of the calculated lifetimes to experiment.<sup>30</sup> Presuming that the decoherence rate does not have a significant temperature dependence, however, the relative change in lifetime at different temperatures should not be affected by the absolute rate of decoherence. Thus, we expect that the temperature-dependent lifetime trends shown in this work can be legitimately compared to experiment.

Pump-probe transient absorption spectra were calculated directly from the electronic energy eigenvalues and transition dipole matrix elements in the simulations in a manner similar to our previous work.<sup>14</sup> Briefly, at each time point, the spectra consisted of a sum of several transitions:

excited-state absorption (from the currently occupied state to higher-lying states, of which 8 were explicitly calculated), stimulated emission (from the currently occupied excited state to the ground state, if the system occupies an excited state), and the ground-state bleach (the negative of the absorption spectrum the system would have had if it had not been excited, as calculated from the original ground-state trajectory). For each component, the calculated energy gaps for all possible transitions were histogrammed into 0.1-eV-width bins, weighted by the corresponding transition dipole matrix elements; the resulting spectra were then convolved in time with a 60-fs-wide Gaussian to represent the experimental instrument response.

Resonance Raman spectra of the LGS and TB hydrated electron models at different temperatures were also calculated as in our previous work.<sup>22</sup> Briefly, we extended the semi-classical method developed by Skinner and co-workers that "maps" the quantum-chemically calculated O–H stretching vibrational frequencies onto the local electric field experienced by the classical water in the simulation.<sup>51–53</sup> It is worth noting that this mapping was developed for pure water<sup>54</sup> and that modifications may be necessary when applying such maps to different systems, such as ionic solutions.<sup>55</sup> Given that we do not have the computational resources to develop a full map for the hydrated electron system, we assumed that the electric field from the hydrated electron contributed equivalently to the electric field from the other water molecules,<sup>54</sup> noting that small differences in the weighting factor would not qualitatively affect any of the conclusions we draw from the Raman spectra calculated below. To simulate resonance Raman rather than bulk Raman spectroscopy, we also weighted the contribution of each water to the spectrum by the square of the force difference projected along the O–H bond between the electronic ground and resonant excited states.<sup>22</sup> For the TB model, we found that generally only the first solvent shell contributed significantly to calculated resonance Raman spectra, while for LGS the main contributions were from the water molecules residing within the electron's radius of gyration.<sup>22</sup> The spectra presented below were averaged inhomogeneously over 200 uncorrelated configurations along each of the various equilibrium ground-state trajectories.

### III. RESULTS AND DISCUSSION

#### A. Temperature dependence of the hydrated electron's structure for cavity and non-cavity models

In order to understand the differences in the hydrated electron's excited-state relaxation with temperature, we begin our study by focusing on the temperature dependence of the ground-state structure. As described above, we ran adiabatic ground-state equilibrium trajectories for both cavity (TB) and non-cavity (LGS) hydrated electron models at several different temperatures ranging from 255 to 350 K. Figure 1 shows electron center-of-mass to water oxygen radial distribution functions for both the LGS [panel (a)] and TB [panel (b)] models. The data make clear that the solvation structure of LGS non-cavity electrons changes noticeably with temperature (the density of water inside 1 Å distance from the electron's center of mass drops by  $\sim 7.5\times$  from 350 to 255 K, as summarized in

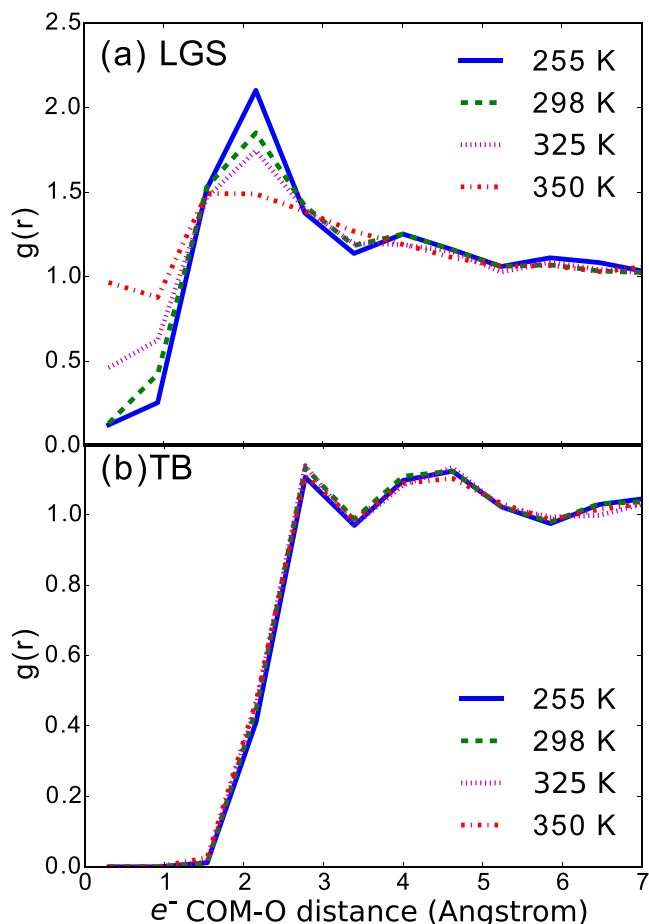


FIG. 1. Temperature dependence of the radial distribution function of the center-of-mass of the hydrated electron to water oxygen for both the (a) LGS non-cavity and (b) TB cavity models. The LGS model shows a clear change in structure with temperature, with the density of waters nearest the center of the electron increasing as the temperature is increased, and the formation of a small central cavity (“hybrid”-like structure) at lower temperatures. In contrast, the TB cavity electron is effectively a hard sphere, showing no change in structure at all over the temperature range investigated.

Table I), while the TB cavity electron’s structure is essentially unaffected by temperature.

For the LGS electron, it is clear that as the temperature is lowered, a small cavity opens near the electron’s center, creating a “hybrid” structure similar to that observed in previous DFT<sup>17</sup> and *ab initio*<sup>18</sup> calculations. This strongly suggests that the driving force for water to enter the electron’s interior is entropic: as the temperature is lowered and entropy becomes less important, the predominantly repulsive enthalpic Pauli exclusion terms in the pseudopotential lead to incipient cavity formation. At higher temperatures, the entropic penalty to expel water from a volume in space is simply too high, so the water penetrates into the electron’s charge density. Given that the LGS model is known to overestimate

the temperature dependence of the electron’s absorption spectrum, this suggests that the LGS model slightly overemphasizes the entropic contributions to the electron’s structure at a given temperature. Thus, it is highly likely that the true structure at room temperature is somewhere between that given by the LGS model and that suggested by “hybrid” models, with the size of the central cavity being highly temperature dependent.

In contrast, the TB model yields the same structure with a  $\sim 2.2$ -Å central cavity independent of the bulk temperature. The change in structure with temperature is so small as to imply that the TB electron is effectively a hard sphere: the repulsive terms in the TB pseudopotential are energetically so steep compared with  $k_B T$  that the relatively modest ( $\sim 30\%$ ) change in absolute temperature we have explored makes effectively no difference in structure. This hard-sphere-like behavior of the TB model indicates that entropy plays almost no role in the observed structure, which is consistent with the fact that the TB model completely misses the known temperature of dependence of the hydrated electron’s absorption spectrum.<sup>22</sup>

The best experimental indicator of the hydrated electron’s structure that we are aware of comes from resonance Raman spectroscopy. Experimentally, the resonance Raman spectrum of the hydrated electron shows a water O–H stretching band that is both broader than and redshifted from that of bulk liquid water.<sup>9</sup> We have shown in a previous work that the TB cavity model predicts a resonance Raman O–H stretch that is narrower and blue-shifted compared with that of bulk water, in sharp contrast to experiment.<sup>22</sup> The predicted narrowing of the band results from the fact that the exterior first-shell waters whose O–H stretches are displaced upon excitation of the TB electron are in roughly equivalent environments, leading to less inhomogeneous broadening. The predicted blue-shift of the TB resonance Raman O–H stretching band results from the fact that the electron is a poorer H-bond acceptor than another water molecule, so that the first-shell water molecules have O–H stretches that are freer than those of bulk water.

The predicted resonance Raman spectrum of the LGS electron, in contrast, is in excellent qualitative agreement with experiment.<sup>22</sup> The broadening of the LGS O–H stretching Raman band results from the fact that the H-bonds of the interior waters can point in any direction with respect to the electric field gradient created by the electron, so that inhomogeneous broadening is enhanced because some waters have their H-bonds strengthened by the electron while others have their H-bonds weakened by the electron. The red-shift of the predicted LGS Raman spectrum results from the fact that the interior waters are packed at a slightly higher density than in bulk water due to electrostriction, leading to an average net strengthening of H-bonds that is similar to what is seen when water is compressed under pressure.<sup>22</sup>

The changes in structure seen in Fig. 1 lead to very definite predictions for the temperature dependence of the O–H stretching line shape of the hydrated electron’s resonance Raman spectrum. Figure 2 displays the calculated Raman spectrum for the LGS non-cavity [panel (a)] and TB cavity [panel (b)] models of the hydrated electron as a function of temperature. Not surprisingly, the predicted Raman spectrum for the TB

TABLE I. Density of water in the vicinity of the electron center-of-mass.

T (K)	255	298	325	350
LGS 1.0 Å	$0.100 \pm 0.213$	$0.276 \pm 0.398$	$0.555 \pm 0.438$	$0.76 \pm 0.36$
LGS 2.45 Å	$1.69 \pm 0.14$	$1.57 \pm 0.13$	$1.51 \pm 0.09$	$1.41 \pm 0.06$
TB 2.45 Å	$0.23 \pm 0.05$	$0.23 \pm 0.05$	$0.26 \pm 0.05$	$0.26 \pm 0.05$

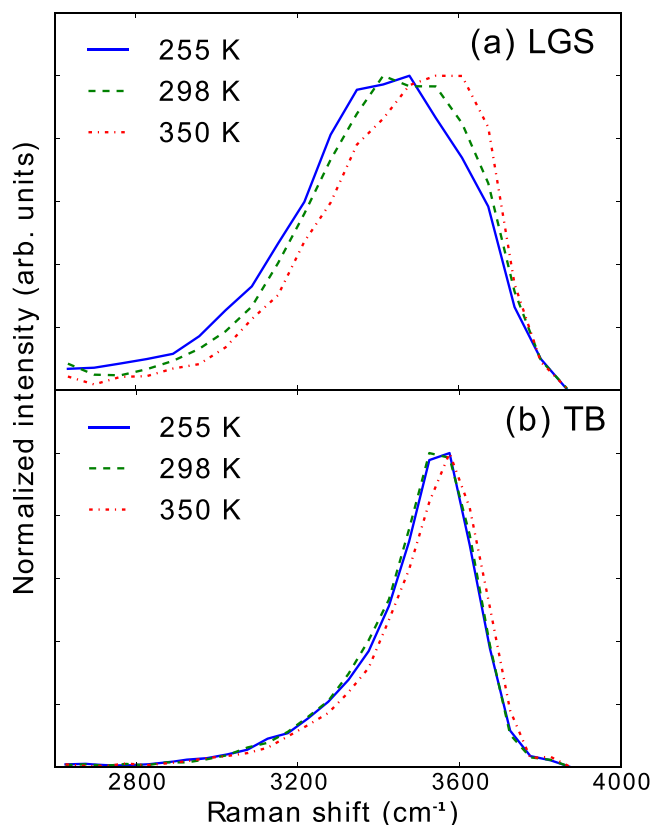


FIG. 2. Temperature dependence of the O–H stretching region of the resonance Raman spectrum of the hydrated electron for both the (a) LGS non-cavity and (b) TB cavity models. The blue-shift of the O–H stretch band of LGS as the temperature is raised reflects the general shift of the bulk water band with increasing temperature and the net decrease in interior water density of the electron (see text and Table I), whereas the lack of structural change of the TB model leads to almost no predicted change in the Raman spectrum with temperature. These disparate simulated predictions—a blue-shifting O–H band or no change whatsoever with increasing temperature—should be directly testable by future temperature-dependent resonance Raman experiments.

model shows virtually no change with temperature, a direct reflection of the fact that the TB electron’s structure is temperature independent. For the LGS model, on the other hand, the prediction is that the O–H stretching Raman band blue-shifts with increasing temperature.

The predicted blue-shift of the LGS electron’s resonance Raman O–H stretch with increasing temperature has two origins. First, the predicted Raman spectrum of the simulated bulk SPC-Flex water blue-shifts with increasing temperature (about twice as much as seen experimentally;<sup>56</sup> see the [supplementary material](#) for details). Since the waters inside the LGS electron maintain a bulk-like environment,<sup>14</sup> their Raman spectrum should also follow this shift. Second, the average interior water density of the LGS hydrated electron changes with temperature, as summarized in Table I. Even though the LGS electron opens a small central cavity at lower temperatures, the total water density inside the electron’s  $\sim 2.5$  Å radius of gyration actually increases at lower temperatures, as can be seen by integrating the radial distribution functions in Fig. 1(a) (it is important to remember that the integrated density measured by  $g(r)$  is weighted by  $r^2$ ). As the temperature is increased, the small “hybrid” central cavity fills in, but the water structure becomes increasingly bulk-like; indeed, the

radial distribution function of the LGS electron at 350 K is nearly flat. Thus, at high temperatures, entropy reduces the electrostriction that increases the interior LGS electron water density, so the calculated resonance Raman spectrum blue-shifts to reflect the more bulk-like environment of the interior water molecules. The breadth of the calculated LGS Raman spectrum does not appear to change significantly with temperature. This is because H-bonds of the interior water molecules continue to point in all directions with respect to the electron’s electric field gradient, so that the electron’s enhancement of the O–H stretch inhomogeneity is not strongly temperature dependent.

Overall, Fig. 2 provides a definite prediction that should be directly testable by experiment: either the resonance Raman spectrum of the electron shows effectively no temperature dependence, consistent with a TB-like cavity picture, or it shows some type of temperature-dependent change in position or width. The LGS-model predicts a noticeable blue-shift with increasing temperature without a significant width change. Although no temperature-dependent calculations have been done to date for “hybrid” models, given that such models have a room temperature structure that is similar to the LGS model at only slightly lower temperatures (and that the LGS model overestimates the temperature dependence), we would expect that “hybrid” models will likely predict a similar temperature-dependence to their Raman spectrum as LGS. Of course, the experimental Raman spectrum may show a different temperature dependence than that predicted here, which would not only invalidate the traditional cavity model but also indicate that the actual entropic contribution to the electron’s ground-state structure is different from that predicted by the LGS and “hybrid” models.

## B. Temperature dependence of cavity and non-cavity hydrated electrons’ excited-state relaxation

When the hydrated electron is excited to one of its electronic excited states by photoexcitation, relaxation takes place on multiple time scales. First, the surrounding water molecules rearrange to accommodate the new structure of the excited-state electron. During the first  $\sim 50$  fs after excitation, the TB cavity model predicts that the occupied excited state increases in energy by  $\sim 200$  meV, while the LGS model predicts that this state undergoes a  $\sim 50$  meV decrease in energy.<sup>30</sup> Experimentally, time-resolved photoelectron spectroscopy (TRPES) experiments show that the occupied excited-state energy slightly decreases following photoexcitation,<sup>57</sup> consistent with the LGS model but not with the cavity picture of the hydrated electron. Second, the excited electron then undergoes internal conversion on a  $\sim 100$ -fs time scale,<sup>12,57,58</sup> the result of a rapid solvent-induced radiationless transition to the ground state. Finally, since the newly created ground-state electron is formed out of equilibrium with the solvent, there is “cooling” of the initially “hot” ground state as the solvent returns the ground-state electron back to equilibrium. Both TRPES experiments and the LGS model indicate that this cooling process takes place in  $\sim 400$  fs, while the TB model predicts significantly faster cooling that is not consistent with the experiment.<sup>30</sup>

Pump-probe transient absorption spectroscopy also has been used extensively to study the excited-state relaxation processes following photoexcitation of the hydrated electron.<sup>3-7,59-61</sup> Like TRPES, pump-probe experiments observe several distinct time scales following photoexcitation, including spectral changes on a 50-100 fs time scale, a  $\sim 450$  fs time scale, and a smaller-amplitude change on a  $\sim 1.1$  ps time scale.<sup>3</sup> Because transient absorption spectroscopy cannot unambiguously determine the electronic state in which the electron resides, two different models have been proposed to interpret the pump-probe data: an “adiabatic” model, where solvation of the excited-state electron takes  $\sim 100$  fs, the subsequent internal conversion takes several hundred fs,<sup>61-63</sup> and ground-state cooling takes  $\sim 1$  ps; and a “nonadiabatic” model, in which the  $\sim 100$ -fs time scale is internal conversion and both of the longer time scales reflect equilibration of the ground state.<sup>59,60</sup> The TRPES experiments discussed above demonstrate clearly that the “non-adiabatic” picture is correct.<sup>12,57,58</sup>

For all of this work exploring the relaxation of the photoexcited hydrated electron, there have been essentially no previous studies, either experimental or theoretical, aimed at understanding the temperature dependence of the electron’s excited-state relaxation. Thus, we begin our exploration of this temperature dependence by exploring the survival probability (i.e., fraction of trajectories remaining in the excited state at a given time after excitation) of both the TB cavity and LGS non-cavity models following simulated photoexcitation. The survival probability data at different temperatures for both models are plotted in Fig. 3. Over the range of temperatures investigated, the average excited-state lifetime for the TB model changes by  $\sim 30\%$ , while that for the LGS non-cavity model changes by over a factor of three: the two models thus predict a temperature dependence that differs by an order of magnitude. For a temperature difference of  $45^\circ\text{C}$ , which we were able to explore experimentally in Paper II,<sup>39</sup> the TB model predicts a  $\leq 20\%$  change in the excited-state lifetime, while the LGS model predicts a lifetime change of just under a factor of two.

Why do the two models predict such starkly different temperature dependencies? Since the two different electron models start with different ground-state structures and the excited-state lifetime of the hydrated electron is  $\sim 100$  fs, there is no time for significant structural rearrangement following vertical excitation. Thus, the different models have different excited-state structures at different temperatures that give rise to internal conversion with different rates. We know from Fig. 1 that the TB electron’s ground-state structure is temperature insensitive, which is consistent with the relative lack of temperature dependence of its excited-state lifetime, whereas the dramatic change with temperature in the predicted excited-state lifetime of the LGS electron makes sense given the strong temperature dependence of its ground-state structure.

This argument still leaves the questions, however, as to what are the excited-state structures that lead to the different predicted temperature dependences for the hydrated electron’s excited-state lifetime? Unfortunately, the fact that the FSSH algorithm we use to compute non-adiabatic dynamics gives

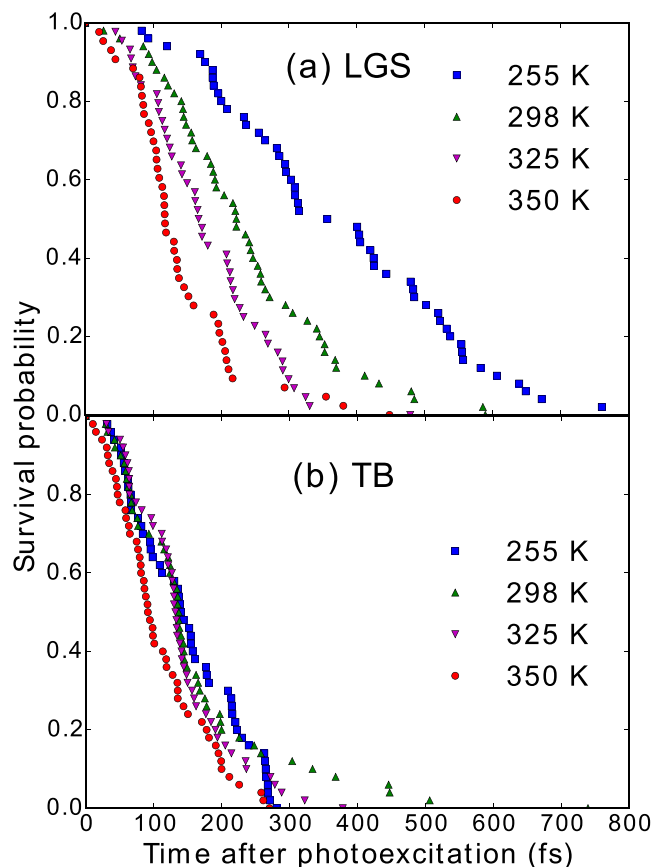


FIG. 3. Survival probability of remaining in the excited state for (a) the LGS non-cavity and (b) the TB cavity hydrated electron models as a function of temperature.

absolute calculated lifetimes for both models that are too long<sup>30</sup> means that the simulations have too much excited-state solvent relaxation prior to the internal conversion. On the other hand, since we know where the structure starts following photoexcitation (Fig. 1), if we can calculate the excited-structure that solvation dynamics is trying to produce (even if the structure is never equilibrated on the excited state because the radiationless transition happens first), we can still meaningfully understand the different predictions for the temperature dependence of the lifetime of the different hydrated electron models.

In Fig. 4, we show the structures of the LGS (top panels) and TB (lower panels) hydrated electrons following equilibration on the lowest excited state (blue curves) at the extremes of our explored temperature range; these structures were computed by averaging over configurations in which the electron had occupied the excited state for at least 500 fs following photoexcitation. The ground-state structures at these same temperatures (green dashed curves) are also shown for comparison. It is worth noting that the excited state of both electrons is  $p$ -like and thus has cylindrical symmetry that is not well-captured by a spherically averaged radial distribution function.<sup>62</sup> Nonetheless, for the TB electron, Fig. 4 shows clearly that the excited state has water molecules occupying what had been the central ground-state cavity. The driving force for this is the fact that the water can best relax around the excited TB electron by moving into the node of the  $p$ -like excited-state wave function.<sup>62</sup>

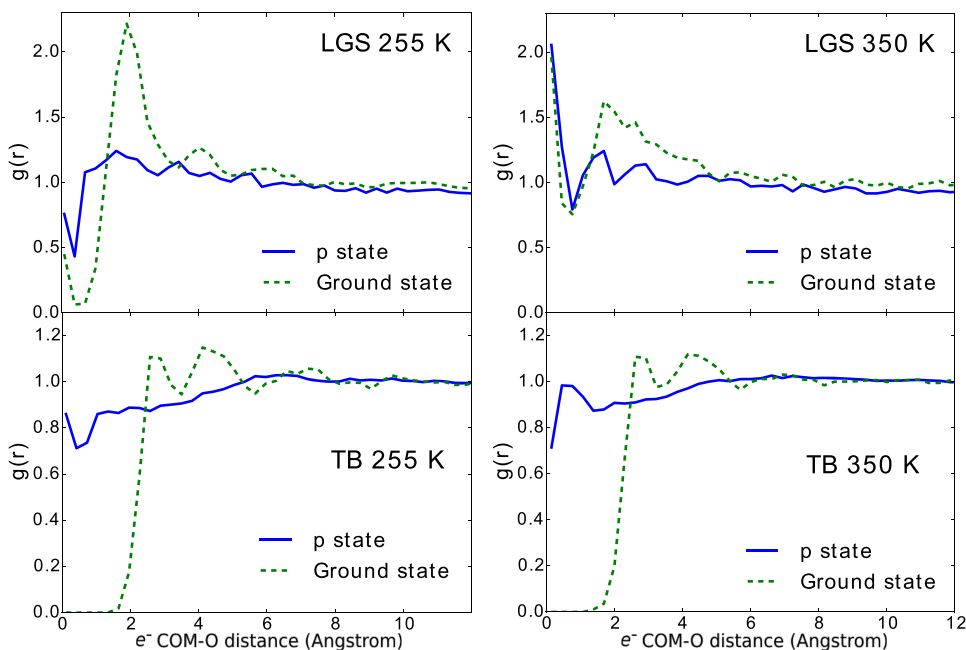


FIG. 4. Radial distribution functions of the center-of-mass of the hydrated electron to water oxygen for both the LGS model (upper panels) and TB models (lower panels) in both the equilibrium ground (green dashed curves, same as Fig. 1) and excited (blue curves) states at both 255 K (left panels) and 350 K (right panels). Like that of the ground state, the LGS excited-state structure has a greater enhancement of water density near the center-of-mass (which helps to induce the non-adiabatic transition to the ground state) at higher temperatures. Also like its ground state, the excited-state structure of the TB electron shows essentially no temperature dependence, explaining why its excited-state lifetime is essentially temperature independent.

Like the ground state, the final equilibrium structure of the TB excited state does not change significantly with temperature, so whatever structural intermediate between the equilibrated ground and excited states is produced when the non-adiabatic transition occurs that structure is essentially the same across the temperature range we have explored.

For the LGS electron, on the other hand, excited-state solvation dynamics work to remove the enhanced water density that resides  $\sim 2$  Å from the electron's center of mass; at lower temperatures, the equilibrium excited-state structure also has a reduced size of the small central ground-state cavity. That said, it is clear from Fig. 4 that the equilibrium excited-state structure of the LGS electron still has a strong temperature dependence: there is still a small (albeit reduced) central cavity at lower temperatures, whereas there is enhanced water density near the electron's center of mass at higher temperatures. The fact that both the starting and ending structures following photoexcitation at different temperatures are different for the LGS electron explains the large temperature dependence of the calculated excited-state lifetime. For example, the difference between the ground- and excited-state structures of the LGS electron is larger at colder temperatures. This means that even if the solvent nuclei were to move the same speed, it will still take longer to reach the conical intersection on the adiabatic manifold at lower temperatures, explaining the longer excited-state lifetime.

Given that the TB model does not change either its ground or excited-state solvation structure when the temperature is changed, why does it show any temperature dependence to its excited-state lifetime at all? We know that the non-adiabatic coupling depends on the nuclear velocity  $\mathbf{v}$  of the solvent molecules that couple the  $|s\rangle$  and  $|p\rangle$  states,

$$\langle s | \frac{\partial |p\rangle}{\partial t} = \langle s | \frac{\partial |p\rangle}{\partial \mathbf{R}} \cdot \frac{\partial \mathbf{R}}{\partial t} = \mathbf{d} \cdot \mathbf{v}, \quad (1)$$

where  $\mathbf{d}$  is the non-adiabatic coupling vector. The velocity term in Eq. (1) is obviously temperature dependent, since

statistically the solvent velocity along any coordinate scales as the square root of the bath temperature. Over the temperature range studied in this work, the solvent velocities change by  $\sim 18\%$ , which explains nearly all of the observed change in the TB electron's lifetime with temperature. Of course, this effect is also present in the temperature dependence of the LGS electron's lifetime, but it is swamped by the larger effect of the temperature-dependent structural change.

The different models' predictions for the temperature dependence of the hydrated electron's lifetime should be directly testable experimentally. Time-resolved photoelectron spectroscopy experiments can directly measure this lifetime,<sup>12,57,58</sup> and it should be readily possible to do these experiments over at least a limited temperature range. Even if the experiments only can be done between temperatures of 0 and 45 °C, as with the transient absorption experiments described in Paper II,<sup>39</sup> the experiments should still easily be able to distinguish the  $\sim 20\%$  change in lifetime predicted by the cavity model versus the factor of  $\sim 2$  change predicted by the non-cavity model. It should also be possible to observe the lifetime change by pump-probe transient absorption spectroscopy, which we turn to in Sec. III C, setting the stage for the analysis of our experiments described in Paper II.<sup>39</sup>

### C. Simulated temperature-dependent transient absorption of cavity and non-cavity hydrated electrons

One of the key differences between TRPES and transient absorption (TA) experiments is that the latter can only probe how the various energy gaps of the hydrated electron change with time; the energy gaps involved in TA can have different dynamics than the energy difference between the occupied state and ionized electron probed in TRPES. Thus, to understand the temperature dependence of transient absorption spectroscopy of the hydrated electron, we need

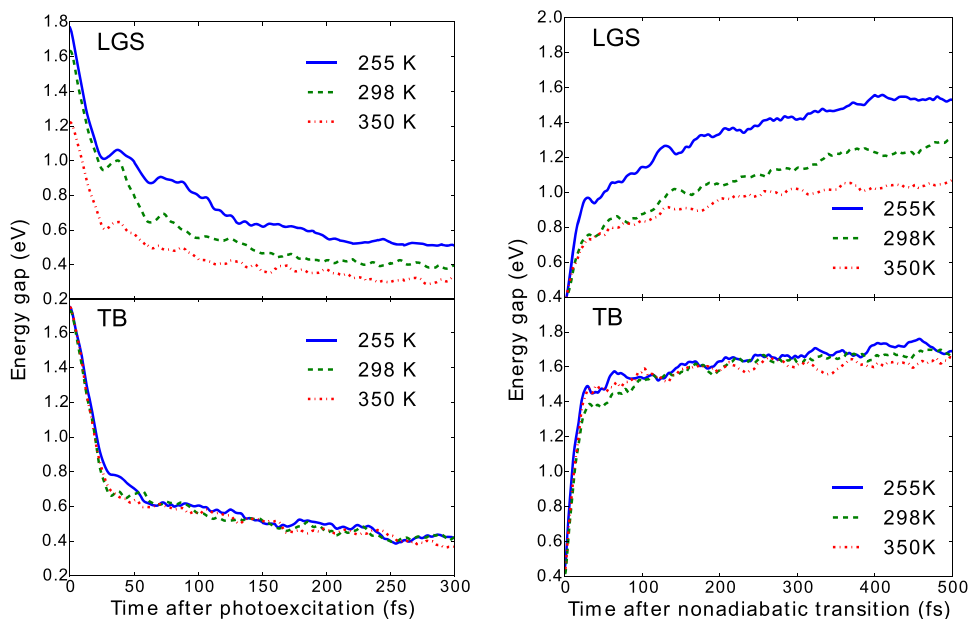


FIG. 5. Temperature dependence of the dynamics of the energy gap between the ground and first electronic excited states of the hydrated electron following photoexcitation (upper panels) and following the non-adiabatic transition to the ground state (lower panels) for both the LGS non-cavity (left panels) and TB cavity (right panels) models. Consistent with the equilibrium ground- and excited-state structures seen in Fig. 4, the LGS electron has different initial and final gaps at different temperatures, as well as different dynamics connecting them, whereas the structural invariance of the TB electron with temperature leads to gap dynamics that are temperature independent. These different predictions should be experimentally testable by TRPES or TA.

to explore how the various energy gaps probed in transient absorption spectroscopy change dynamically with temperature, which are shown for the LGS model (left panels) and TB model (right panels) in Fig. 5. The upper panels of this figure show the dynamics of the energy gap between the ground and first excited states while the electron occupies the excited state following photoexcitation, and the lower panels show the same energy gap while the electron occupies the ground state as a function of time following the non-adiabatic transition.

For LGS, the initial gap after excitation (time zero in the upper left panel) and the equilibrated gap after non-adiabatic relaxation (long times in the lower left panel) are clearly temperature dependent, as reflected in the known (and admittedly somewhat exaggerated) temperature dependence of the equilibrium absorption spectrum of this model,<sup>22</sup> reflecting the structural changes with temperature seen in Figs. 1 and 4. More importantly, the figure makes clear that although the gap closing dynamics during the  $\sim 100$  fs the electron occupies the excited state are not strongly temperature dependent, the relaxation dynamics following the non-adiabatic transition (upper right panel of Fig. 1) are somewhat temperature dependent: the gap closing accompanying the ground-state cooling is a bit faster and has a smaller amplitude at higher temperatures, and is somewhat slower with a larger amplitude at colder temperatures. The smaller amplitude at higher temperatures is a result of the fact that the system is recovering to a smaller equilibrium energy gap, but the faster dynamics result from the fact that the underlying solvent motions that close the gap are faster at higher temperatures.

In contrast, the equilibrium gap for the TB model (lower left panel in Fig. 5) shows no temperature dependence, as expected from the complete lack of a temperature-dependent structural change, which is also why the equilibrium absorption spectrum does not change with temperature.<sup>22</sup> But perhaps even more strikingly, Fig. 5 shows that none of the gap dynamics, either after photoexcitation or following non-adiabatic relaxation, have any significant temperature dependence. This

means that in addition to the excited-state lifetime, the TB electron should show no temperature dependence for any of its excited-state relaxation processes, including the ground-state cooling. Part of the reason for this is that the energy gap relaxations for the TB electron are dominated by inertial water motions<sup>30</sup> whose dynamics do not change much with temperature (at most by the  $\sim 18\%$  change in average librational velocity over the temperature range studied). But even the longer time scale diffusive motions show little temperature dependence for the TB electron, again marking an experimentally determinable contrast between the cavity and non-cavity pictures of the hydrated electron.

Now that we understand how the dynamics of the energy gaps change with temperature, we can turn to studying the full temperature-dependent pump-probe transient absorption spectra for both the cavity and non-cavity models of the hydrated electron. In Fig. 6, we show the calculated transient absorption spectra at different temperatures for the LGS non-cavity (left panels) and the TB cavity (right panels) models in the energy range of the transient absorption spectra that we study experimentally in Paper II.<sup>39</sup> For the spectral region plotted in Fig. 6, the calculated transient absorption spectra consist mostly of the ground-state bleach, along with contributions from stimulated emission at early times, and the recovering hot ground state absorption that fills in the bleach at later times. We show the individual components that contribute to the calculated transient absorption spectra in the [supplementary material](#). The predicted transient absorption contours for both models are not perfectly smooth because the non-equilibrium ensemble we average over is not large enough to average out the phase of low-frequency oscillatory motions that are impulsively driven upon excitation.<sup>14,30,62,63</sup>

As expected from what is known about the temperature dependence of their ground-state absorption spectra,<sup>22</sup> the peak bleach (purple/blue contours) of the LGS electron's transient absorption at early times red-shifts with increasing temperature, while that for the TB electron is constant with temperature. For the LGS model, the ground-state

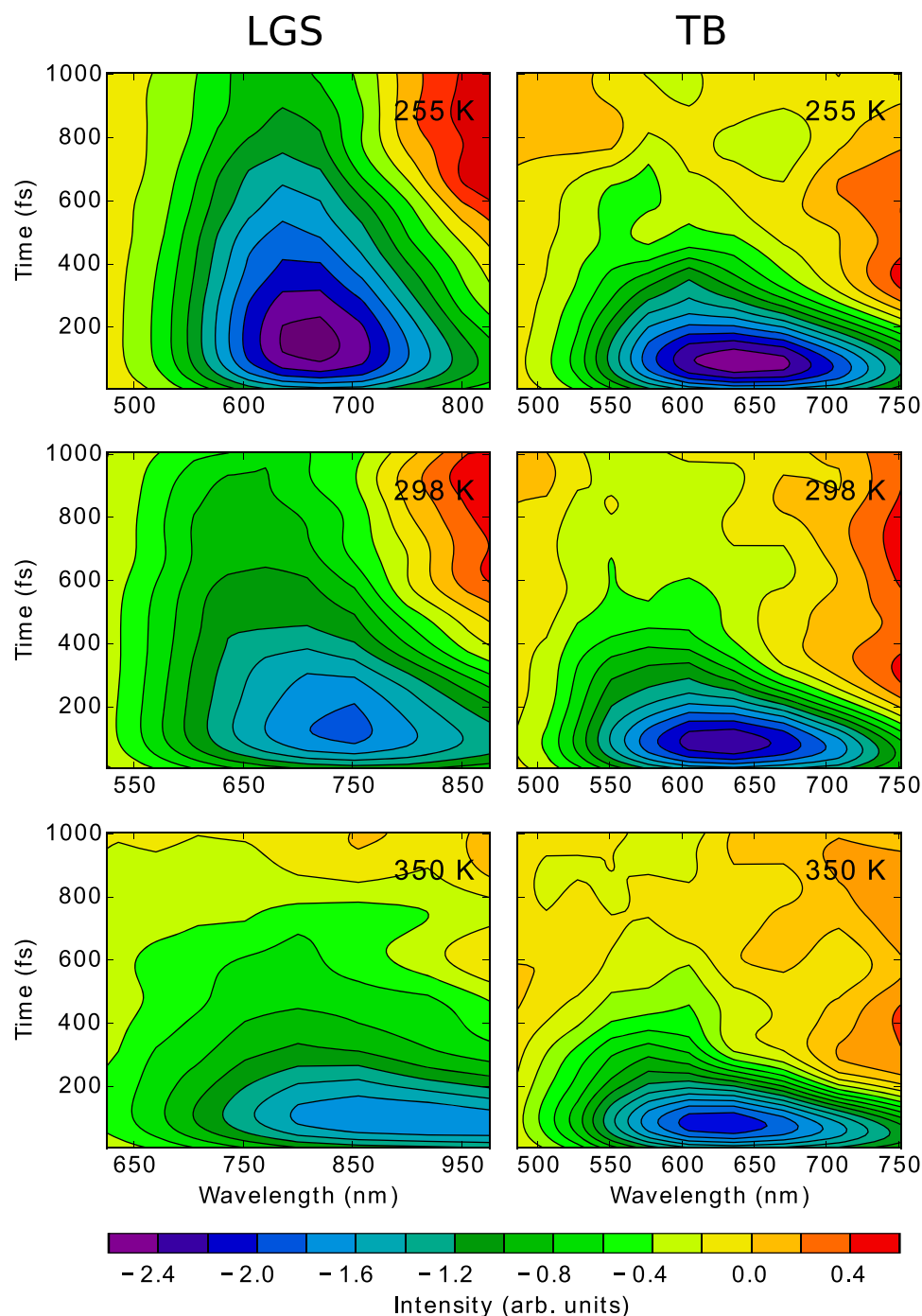


FIG. 6. Calculated broadband transient absorption spectra for the LGS non-cavity (left panels) and TB cavity (right panels) hydrated electron models at 255 K (top panels), 298 K (center panels), and 350 K (lower panels). For LGS, in addition to the fact that the early time bleach is red-shifted, the kinetics at which the bleach blue-shifts and recovers are faster at higher temperatures, in reasonable agreement with the experiments in Paper II.<sup>39</sup> For TB, the calculated transient absorption signals at the three different temperatures are the same within the error, which along with the very rapid blue-shift of the maximum bleach is in contrast to experiment; see Paper II<sup>39</sup> for details.

absorption is homogeneously broadened,<sup>14,30</sup> so the ground-state bleach is identical within the noise to the equilibrium absorption spectrum. For the TB electron, on the other hand, the ground-state absorption spectrum is inhomogeneously broadened, leading to the possibility of spectral diffusion in the bleach if polarized pump and probe pulses are employed to suppress electronic “replica holes.”<sup>37,64,65</sup> We have ignored the relative polarizations of the pump and probe pulses when calculating the transient absorption spectra in this paper, making them effectively unpolarized and thus allowing the initial bleach of the TB electron’s absorption spectrum to match that of its ground-state absorption spectrum. In Paper II,<sup>39</sup> even though it has been demonstrated experimentally that there is no polarization dependence to the observed

transient absorption signals so that the absorption spectrum is homogeneously broadened,<sup>66–68</sup> we perform our temperature-dependent experiments on the hydrated electron using pump and probe pulses with relative polarizations at the magic angle to allow for a direct comparison to the calculations in Fig. 6.

For both hydrated electron models, once the excited-state electron undergoes the internal conversion to the ground state, a hot ground-state electron is produced that absorbs to the red of the equilibrium ground state. As the hot ground state cools, its absorption shifts to the blue with time, where it starts filling in the red edge of the ground-state bleach, leading to an apparent blue-shift of the bleach maximum with increasing time. For the LGS electron, the rate of the bleach

recovery and blue-shift both increase with increasing temperature. This is both because the excited-state lifetime is shorter at higher temperatures (cf. Fig. 3) and because the energy gap associated with ground-state cooling is also smaller at higher temperatures (cf. Fig. 5). In contrast, for the TB model, neither the lifetime nor the cooling rate of the hot ground state changes with temperature, and indeed the predicted transient absorption spectra are identical at all three temperatures within the noise. Although neither model agrees quantitatively with the experimental temperature-dependent transient absorption spectra presented in Paper II<sup>39</sup> (mostly because of the overestimated lifetime in the simulations), a quick comparison of Figs. 6 and 1 in Paper II<sup>39</sup> shows that there is an excellent qualitative match between the LGS model and experiment, and qualitative disagreement with the TB model, for which the calculated blue-shift is both not temperature dependent and too fast compared with experiment.

In their experimental studies of the resonance Raman spectrum, Tauber and Mathies observed fluorescence coming from the photoexcited hydrated electron.<sup>69</sup> Even though simulations predict a very rapid Stokes shift for emission from

the hydrated electron (cf. Fig. 5, which shows a  $\sim 0.6$  eV gap closing for LGS and a  $\sim 1.0$  eV gap shift for TB in the first  $\sim 30$  fs),<sup>63,70</sup> the experimental fluorescence spectrum still shows significant emission just to the red of the excitation wavelength in the visible and near-IR spectral regions, overlapping the ground-state bleach. Thus, it is certainly possible that there could be a stimulated emission component in transient absorption spectroscopy of the hydrated electron in the region of the bleach at early times, as has been speculated in previous experimental work.<sup>4,6,71</sup>

To investigate how such a stimulated emission component would be manifest spectroscopically, we plot the early time transient absorption spectra for both hydrated electron models as a function of temperature in Fig. 7 in a different way: we normalize the spectra at each time on the blue edge, where the only spectral component that contributes is the ground-state bleach (various colored, dashed curves). In this way, any differences seen from one time to the next must be the result of stimulated emission or the hot recovering ground state, since excited-state absorption plays little role in this spectral window. To help with the comparison, the black solid curve in each panel shows the (negative of the) equilibrium absorption spectrum

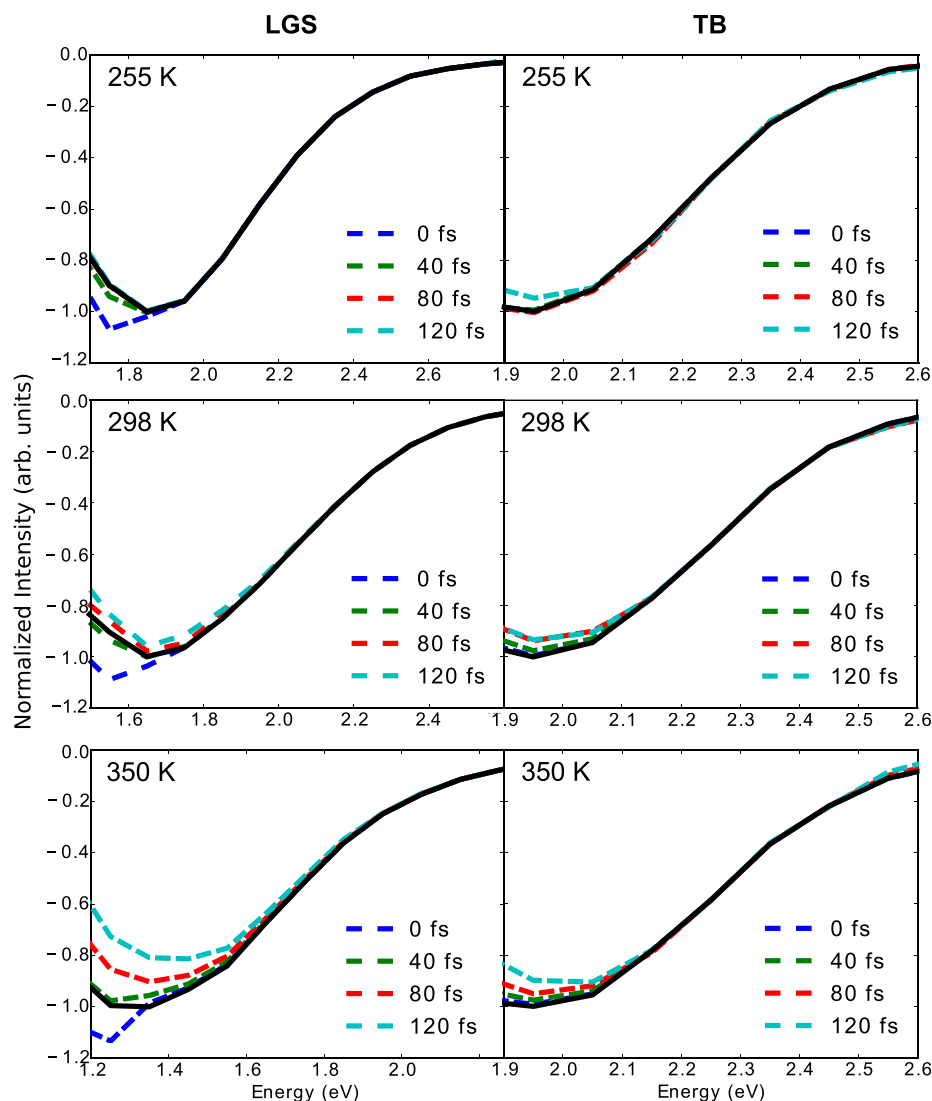


FIG. 7. Early time calculated transient absorption spectroscopy of both the LGS and TB hydrated electron models, normalized in the blue region of the spectrum so that the underlying ground-state bleach has a constant amplitude; the black solid curve shows the (negative of the) equilibrium absorption spectrum that is equivalent to the homogeneously broadened bleach. The temperature dependence of the observed stimulated emission amplitude and decay dynamics for the LGS model are in excellent agreement with the experiments in Paper II,<sup>39</sup> while the lack of any excess bleach component predicted by the TB model runs counter to experiment.

spectrum, which is equivalent to the homogeneously broadened bleach.

The excess bleach seen at the red edge of our spectra window at early times for LGS on the left side of Fig. 7 results from stimulated emission (see the [supplementary material](#)), as there is no other mechanism that can lead to an enhanced negative absorption signal. The loss of the LGS electron's stimulated emission/excess bleach with time is due to a combination of the Stokes shift of the stimulated emission out of the probe window, the decay of the stimulated emission due to the electron's excited-state lifetime, and the presence of the hot ground-state absorption that shifts into the spectral window from the red as the recovering electron cools. Because both the excited-state lifetime (Fig. 3) and the cooling of the hot ground state (Fig. 5) are faster at higher temperatures for the LGS electron, the excess bleach/stimulated emission feature also decays faster at higher temperatures. The presence of stimulated emission and its temperature dependence predicted here for LGS are in excellent agreement with what we observe experimentally in Fig. 3 of Paper II.<sup>39</sup>

In contrast to both the LGS model and experiment, the TB model predicts no observable stimulated emission/excess bleach at early times. This is because the Stokes shift of the excited hydrated electron's emission during the  $\sim 35$ -fs inertial relaxation is nearly twice as large for the TB model than for the LGS model, and because the cooling of the TB electron's hot ground state is more than four times faster than that of the LGS model (cf. Fig. 5).<sup>30</sup> Thus, even though the simulations predict that there is indeed a small stimulated emission component at early times in this spectral window for the TB model (see the [supplementary material](#)), the amplitude is small enough compared with that of the ground-state bleach and the blue tail of the most rapidly produced hot ground-state electrons as to not be distinguishable with the  $\sim 60$ -fs time resolution simulated here. The rapid Stokes shift of the TB model also would predict a much more red-shifted fluorescence spectrum than is seen experimentally.<sup>69</sup>

#### D. Modeling the transient absorption spectroscopy: The effective temperature of the hot ground-state electron

As discussed in more detail in Paper II,<sup>39</sup> the interpretation of the pump-probe transient absorption spectroscopy of the hydrated electron requires a kinetic model to extract the various relaxation time scales from experimental data. Modeling the excited-state absorption and Stokes shift of the stimulated emission is quite complex, but for the visible region of the spectrum, there is at least a simple model that can be employed to account for the cooling of the hot ground state that leads to recovery of the ground-state bleach.<sup>3</sup> The basic idea is to model the spectrum of the hot ground state as being at quasi-equilibrium, with a temperature higher than that of the bulk. Since the temperature dependence of the hydrated electron's absorption spectrum is known experimentally,<sup>8</sup> this means that the entire ground-state cooling process can then be described by only 2 parameters. These are a temperature jump,  $\Delta T$ , which characterizes the initial spectrum of the hot ground state immediately following the non-adiabatic transition, and a cooling time,  $\tau_{\text{cool}}$ , by which the temperature describing the

hot electron's spectrum relaxes exponentially back to the equilibrium bulk temperature (some workers use a bi-exponential with two cooling times to model the temperature relaxation).<sup>4</sup> Of course, such models presume that the hot ground-state electron, which is clearly a nonequilibrium object, has a spectrum that can be well approximated by an equilibrium spectrum at a higher temperature.

As discussed in Paper II,<sup>39</sup> when fitting standard kinetic models to pump-probe transient absorption spectroscopy of the hydrated electron at room temperature, the excited-state lifetime and  $\Delta T$  parameters are highly correlated. In fact, fits with a lifetime of 300-400 fs and a temperature jump of  $\sim 30$  K are about as good as fits with a lifetime of  $\geq 100$  fs and a  $\Delta T$  of a few hundred K. One of the arguments in favor of the so-called "adiabatic" relaxation model, with the longer lifetime, was that the temperature jump of  $\sim 30$  K made much more physical sense than a jump an order of magnitude larger (based on the argument that  $\sim 30$  K is about what is expected if the non-adiabatic transition releases 0.5 to 1.0 eV of energy spread statistically among a few dozen nearby water molecules). Of course, as discussed above, TRPES experiments have shown that the excited-state lifetime of the electron is short, falling squarely into the "non-adiabatic" relaxation picture.<sup>12,57,58</sup> This then leaves the question of whether or not it makes sense to model the relaxation of the hot ground state using the temperature dependence of the equilibrium spectrum extrapolated to a few hundred K above room temperature.

Fortunately, in our simulations, it is straightforward to calculate the spectrum of the hydrated electron's hot ground state immediately after the non-adiabatic transition takes place. The red curves in Fig. 8 show the calculated immediately-produced hot ground-state spectrum for both the LGS non-cavity [panel (a)] and the TB cavity [panel (b)] models of the hydrated electron. The spectra shown are for photoexcitation from a bulk temperature of 298 K, but the hot ground state spectra of both models do not change within error over the entire equilibrium temperature range that we explored. For the LGS model, the hot ground-state is substantially red-shifted from that at equilibrium (blue curve). If this were an equilibrium spectrum and we extrapolate using the temperature dependence of the LGS model seen in our previous work,<sup>22</sup> the hot ground state would be at a temperature  $\sim 120$  K hotter than the bulk temperature. For the TB model, the hot ground-state is also red-shifted from the bulk but much less than that for the LGS model. Of course, the TB model has almost no temperature dependence to its absorption spectrum,<sup>22,33</sup> so this modest red-shift would be equivalent to a temperature jump of over 500 K for the TB model.

Overall, the data in Fig. 8 indicate that the nonequilibrium hydrated electron's hot ground state is reasonably well approximated by an equilibrium spectrum, but at an unphysically large temperature. The need for such a large temperature jump should not be taken to imply that the water surrounding the hot ground state electron is actually at a very high temperature; instead, the data simply indicate that the situation is so far from equilibrium that the best parameter to use in an equilibrium approximation corresponds to a very large increase in temperature. Thus, the fact that the experimental data in Paper II<sup>39</sup> fit well to the model with a  $\Delta T$  of  $\sim 250$  K suggest

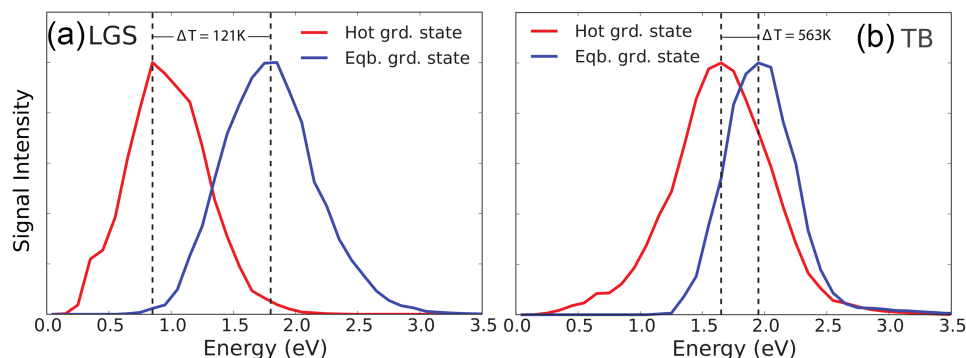


FIG. 8. The spectrum of the hot ground state of the hydrated electron produced immediately following the non-adiabatic transition (red curves) compared to the equilibrium ground-state absorption spectrum (blue curves) for the (a) LGS non-cavity and (b) TB cavity models with the bulk system at room temperature. The LGS electron's hot ground state spectrum is quite red-shifted from the equilibrium spectrum, corresponding to an effective temperature increase of at least 120 K. The TB electron's hot ground-state shows only a modest spectral red-shift, but since the TB model has almost no temperature dependence, this modest redshift corresponds to a temperature jump of over 500 K. For both models, it is clear that the hot ground-state electron is far out of equilibrium, so that the best equilibrium condition that can be used to approximate the nonequilibrium state corresponds to an unphysically high temperature.

that the simulations do indeed capture this aspect of the experiment and that experimental fits that give large temperature jumps are not in fact unphysical.

#### IV. CONCLUSIONS

In summary, we have studied the relaxation dynamics of the photoexcited hydrated electron as a function of temperature using mixed quantum/classical simulations. Our calculations offer concrete predictions for the results of future experiments that could possibly distinguish between the traditional cavity picture of the hydrated electron, exemplified here by the TB pseudopotential model, and our more recent non-cavity picture produced by the LGS pseudopotential model. We find that cavity models of the hydrated electron show no change in the ground-state structure with temperature, whereas the non-cavity model predicts that significant structural changes occur as the temperature is varied. For the non-cavity model, colder temperatures lead to the production of a small central cavity but also increase the water density within the electron's radius of gyration. At higher temperatures, the non-cavity electron causes less disruption of the structure of liquid water. The non-cavity model at cooler temperatures shows a similar structure to "hybrid" models based on DFT<sup>17</sup> or *ab initio*<sup>18</sup> calculations, suggesting that these models may in fact be roughly equivalent other than slight differences in the exact temperatures at which the various structural changes take place, particularly given that the LGS non-cavity model we use here is known to overestimate the experimental temperature dependence of the ground-state absorption spectrum.

The way each model's structure changes with temperature leads to definite predictions for the results of future temperature-dependent resonance Raman experiments. The lack of temperature-dependent structural change for cavity models of the hydrated electron explains why such models predict that there would be essentially no change in the resonance Raman spectrum with temperature at constant density; the lack of structural change with temperature also predicts that the ground-state electronic absorption spectrum at constant density is temperature-invariant (a result at odds with experiment<sup>8,31,32</sup>). In contrast, the blue-shift of the bulk water

Raman spectrum with increasing temperature and the lowering of the overall interior density seen with the non-cavity model as the temperature is increased suggest that the O–H stretch of the hydrated electron's resonance Raman spectrum should blue-shift with increasing temperature at constant density.

The temperature-dependent structural differences of the cavity and non-cavity models also lead to definite predictions for the excited-state relaxation dynamics of the hydrated electron. Since the structure of the cavity model is essentially temperature invariant, the only thing that can affect the excited-state lifetime of the electron is the fact that the water motions that cause internal conversion are slightly faster at higher temperatures, leading to a very mild decrease in lifetime as the temperature is increased ( $\sim 10\%$  over a  $\sim 50$  K temperature increase). The cavity model also predicts essentially no change in the time for cooling of the hot ground-state electron produced subsequent to the internal conversion. In contrast, the temperature-dependent ground- and excited-state structures of the non-cavity model of the hydrated electron lead to different dynamics following photoexcitation, so that both the excited-state lifetime and hot ground-state cooling times are predicted to decrease significantly with increasing temperature ( $\sim 2\times$  decrease in lifetime over a  $\sim 50$  K increase). These predictions should be directly testable by future temperature-dependent time-resolved photoelectron spectroscopy experiments.

Finally, the two models also predict significant differences in temperature-dependent pump-probe transient absorption spectroscopy of the hydrated electron, experiments that we carried out subsequent to these predictions and which are described in Paper II.<sup>39</sup> The changing lifetime and ground-state cooling times predicted by the non-cavity model lead to direct signatures in transient absorption spectroscopy that are observed by experiment nearly as predicted here. Moreover, the non-cavity model also predicts the presence of stimulated emission at early times in transient spectroscopy, with both the amplitude and lifetime of the stimulated emission decreasing with increasing temperature, again almost exactly as observed by experiment. In contrast, the cavity model of the hydrated electron predicts almost no change in transient

spectroscopy with temperature and no signs of stimulated emission at early times, features that are both in contrast with experiment. For both models, the simulations show clearly that the hot ground-state electron produced after the radiationless transition from the excited state is far out of equilibrium, so that modeling this species assuming the electron is at equilibrium but at a higher temperature requires the use of an unphysically high temperature, as is also observed experimentally.

Overall, it is clear that one-electron models of the hydrated electron, whether they produce cavity or non-cavity structures, cannot explain all of the known properties of this simplest of quantum solutes. Ultimately, it will be left to *ab initio* calculations to fully cement the connection between a microscopic structural picture of the hydrated electron and its behavior in the myriad experiments whose results have been reported in the literature. But since the use of many-electron simulations to calculate ensembles of non-adiabatic excited-state trajectories with hundreds of water molecules plus an excess electron at several bulk temperatures is presently out of computational reach, we can still take advantage of one-electron models to make definitive predictions for future experiments that will help us to refine our understanding of the possible structures of the hydrated electron. Our conclusion based on comparing the results of these simulations to experiment is that there must be some type of structural change of the electron involving the density of interior water molecules as a function of temperature and that non-cavity or “hybrid” models capture this temperature-dependent structural change better than the more traditional cavity picture.

## SUPPLEMENTARY MATERIAL

See [supplementary material](#) for further details of sample non-equilibrium trajectories and individual components to the transient absorption spectra, and further discussions on the temperature dependence of non-adiabatic dynamics.

## ACKNOWLEDGMENTS

This work was supported by the National Science Foundation under Grant No. CHE-1565434.

- <sup>1</sup>B. C. Garrett, D. A. Dixon, D. M. Camaioni, D. M. Chipman, M. A. Johnson, C. D. Jonah, G. A. Kimmel, J. H. Miller, T. N. Rescigno, and P. J. Rossky, *Chem. Rev.* **105**, 355 (2005).
- <sup>2</sup>J. Gu, J. Leszczynski, and H. F. Schaefer III, *Chem. Rev.* **112**, 5603 (2012).
- <sup>3</sup>K. Yokoyama, C. Silva, D. H. Son, P. K. Walhout, and P. F. Barbara, *J. Phys. Chem. A* **102**, 6957 (1998).
- <sup>4</sup>M. Assel, R. Laenen, and A. Laubereau, *Chem. Phys. Lett.* **317**, 13 (2000).
- <sup>5</sup>A. Hertwig, H. Hippler, and A.-N. Unterreiner, *Phys. Chem. Chem. Phys.* **4**, 4412 (2002).
- <sup>6</sup>A. Thaller, R. Laenen, and A. Laubereau, *Chem. Phys. Lett.* **398**, 459 (2004).
- <sup>7</sup>M. S. Pshenichnikov, A. Baltuška, and D. A. Wiersma, *Chem. Phys. Lett.* **389**, 171 (2004).
- <sup>8</sup>D. Madsen, C. L. Thomsen, J. Thøgersen, and S. R. Keiding, *J. Chem. Phys.* **113**, 1126 (2000).
- <sup>9</sup>M. J. Tauber and R. A. Mathies, *Chem. Phys. Lett.* **354**, 518 (2002).
- <sup>10</sup>A. E. Bragg, J. R. R. Verlet, A. Kammrath, O. Cheshnovsky, and D. M. Neumark, *Science* **306**, 669 (2004).
- <sup>11</sup>D. M. Bartels, K. Takahashi, J. A. Cline, T. W. Marin, and C. D. Jonah, *J. Phys. Chem. A* **109**, 1299 (2005).
- <sup>12</sup>M. H. Elkins, H. L. Williams, A. T. Shreve, and D. M. Neumark, *Science* **342**, 1496 (2013).
- <sup>13</sup>L. Turi and D. Borgis, *J. Chem. Phys.* **117**, 6186 (2002).
- <sup>14</sup>R. E. Larsen, W. J. Glover, and B. J. Schwartz, *Science* **329**, 65 (2010).
- <sup>15</sup>J. M. Herbert and L. D. Jacobson, *J. Phys. Chem. A* **115**, 14470 (2011).
- <sup>16</sup>L. Turi and P. J. Rossky, *Chem. Rev.* **112**, 5641 (2012).
- <sup>17</sup>F. Uhlig, O. Marsalek, and P. Jungwirth, *J. Phys. Chem. Lett.* **3**, 3071 (2012).
- <sup>18</sup>A. Kumar, J. A. Walker, D. M. Bartels, and M. D. Sevilla, *J. Phys. Chem. A* **119**, 9148 (2015).
- <sup>19</sup>L. Kevan, *Acc. Chem. Res.* **14**, 138 (1981).
- <sup>20</sup>C.-G. Zhan and D. A. Dixon, *J. Phys. Chem. B* **107**, 4403 (2003).
- <sup>21</sup>P. J. Rossky and J. Schnitker, *J. Phys. Chem.* **92**, 4277 (1988).
- <sup>22</sup>J. R. Casey, R. E. Larsen, and B. J. Schwartz, *Proc. Natl. Acad. Sci. U. S. A.* **110**, 2712 (2013).
- <sup>23</sup>J. R. Casey, A. Kahros, and B. J. Schwartz, *J. Phys. Chem. B* **117**, 14173 (2013).
- <sup>24</sup>L. Turi and Á. Madarász, *Science* **331**, 1387 (2011).
- <sup>25</sup>L. D. Jacobson and J. M. Herbert, *Science* **331**, 1387 (2011).
- <sup>26</sup>R. E. Larsen, W. J. Glover, and B. J. Schwartz, *Science* **331**, 1387 (2011).
- <sup>27</sup>L. Turi, *J. Chem. Phys.* **144**, 154311 (2016).
- <sup>28</sup>J. R. Casey, B. J. Schwartz, and W. J. Glover, *J. Phys. Chem. Lett.* **7**, 3192 (2016).
- <sup>29</sup>C. D. Borsarelli, S. G. Bertolotti, and C. M. Previtali, *Photochem. Photobiol.* **2**, 791 (2003).
- <sup>30</sup>C.-C. Zho and B. J. Schwartz, *J. Phys. Chem. B* **120**, 12604 (2016).
- <sup>31</sup>F.-Y. Jou and G. R. Freeman, *J. Phys. Chem.* **81**, 909 (1977).
- <sup>32</sup>F.-Y. Jou and G. R. Freeman, *J. Phys. Chem.* **83**, 2383 (1979).
- <sup>33</sup>C. Nicolas, A. Boutin, B. Lévy, and D. Borgis, *J. Chem. Phys.* **118**, 9689 (2003).
- <sup>34</sup>Y. Du, E. Price, and D. M. Bartels, *Chem. Phys. Lett.* **438**, 234 (2007).
- <sup>35</sup>A. Wallqvist, G. Martyna, and B. Berne, *J. Phys. Chem.* **92**, 1721 (1988).
- <sup>36</sup>W. J. Glover and B. J. Schwartz, *J. Chem. Theory Comput.* **12**, 5117 (2016).
- <sup>37</sup>I. A. Shkrob, W. J. Glover, R. E. Larsen, and B. J. Schwartz, *J. Phys. Chem. A* **111**, 5232 (2007).
- <sup>38</sup>F. Uhlig, J. M. Herbert, M. P. Coons, and P. Jungwirth, *J. Phys. Chem. A* **118**, 7507 (2014).
- <sup>39</sup>E. P. Farr, C.-C. Zho, J. R. Challa, and B. J. Schwartz, *J. Chem. Phys.* **147**, 074504 (2017).
- <sup>40</sup>R. E. Larsen, M. J. Bedard-Hearn, and B. J. Schwartz, *J. Phys. Chem. B* **110**, 20055 (2006).
- <sup>41</sup>W. J. Glover, J. R. Casey, and B. J. Schwartz, *J. Chem. Theory Comput.* **10**, 4661 (2014).
- <sup>42</sup>K. Toukan and A. Rahman, *Phys. Rev. B* **31**, 2643 (1985).
- <sup>43</sup>D. J. Evans and B. L. Holian, *J. Chem. Phys.* **83**, 4069 (1985).
- <sup>44</sup>J. C. Phillips and L. Kleinman, *Phys. Rev.* **116**, 287 (1959).
- <sup>45</sup>M. L. Cohen and V. Heine, *Solid State Phys.* **24**, 37 (1970).
- <sup>46</sup>L. Szasz, *Pseudopotential Theory of Atoms and Molecules* (John Wiley and Sons, 1985).
- <sup>47</sup>O. Steinhauser, *Mol. Phys.* **45**, 335 (1982).
- <sup>48</sup>J. C. Tully, *J. Chem. Phys.* **93**, 1061 (1990).
- <sup>49</sup>D. Borgis, P. J. Rossky, and L. Turi, *J. Phys. Chem. Lett.* **8**, 2304 (2017).
- <sup>50</sup>M. J. Bedard-Hearn, R. E. Larsen, and B. J. Schwartz, *Phys. Rev. Lett.* **97**, 130403 (2006).
- <sup>51</sup>S. A. Corcelli, C. P. Lawrence, and J. L. Skinner, *J. Chem. Phys.* **120**, 8107 (2004).
- <sup>52</sup>S. A. Corcelli and J. L. Skinner, *J. Phys. Chem. A* **109**, 6154 (2005).
- <sup>53</sup>R. Kumar, J. R. Schmidt, and J. L. Skinner, *J. Chem. Phys.* **126**, 204107 (2007).
- <sup>54</sup>Y.-S. Lin, B. Auer, and J. Skinner, *J. Chem. Phys.* **131**, 144511 (2009).
- <sup>55</sup>K. Kwac and E. Geva, *J. Phys. Chem. B* **116**, 2856 (2012).
- <sup>56</sup>A. Sokołowska, *J. Raman Spectrosc.* **20**, 779 (1989).
- <sup>57</sup>S. Karashima, Y.-i. Yamamoto, and T. Suzuki, *Phys. Rev. Lett.* **116**, 137601 (2016).
- <sup>58</sup>M. H. Elkins, H. L. Williams, and D. M. Neumark, *J. Chem. Phys.* **144**, 184503 (2016).
- <sup>59</sup>J. C. Alfano, P. Walhout, Y. Kimura, and P. F. Barbara, *J. Chem. Phys.* **98**, 5996 (1993).
- <sup>60</sup>Y. Kimura, J. C. Alfano, P. Walhout, and P. F. Barbara, *J. Phys. Chem.* **98**, 3450 (1994).
- <sup>61</sup>C. Silva, P. K. Walhout, K. Yokoyama, and P. F. Barbara, *Phys. Rev. Lett.* **80**, 1086 (1998).
- <sup>62</sup>B. J. Schwartz and P. J. Rossky, *J. Chem. Phys.* **101**, 6902 (1994).
- <sup>63</sup>B. J. Schwartz and P. J. Rossky, *J. Chem. Phys.* **101**, 6917 (1994).
- <sup>64</sup>J. Yu and M. Berg, *J. Phys. Chem.* **97**, 1758 (1993).

<sup>65</sup>B. J. Schwartz and P. J. Rossky, *Phys. Rev. Lett.* **72**, 3282 (1994).

<sup>66</sup>M. J. Tauber and R. A. Mathies, *J. Chem. Phys.* **125**, 1394 (2003).

<sup>67</sup>M. C. Cavanagh, I. B. Martini, and B. J. Schwartz, *Chem. Phys. Lett.* **396**, 359 (2004).

<sup>68</sup>I. A. Shkrob, *Chem. Phys. Lett.* **467**, 84 (2008).

<sup>69</sup>M. J. Tauber and R. A. Mathies, *J. Phys. Chem. A* **105**, 10952 (2001).

<sup>70</sup>B. J. Schwartz and P. J. Rossky, *J. Phys. Chem.* **99**, 2953 (1995).

<sup>71</sup>A. Baltuska, M. Pshenichnikov, and D. Wiersma, in *Quantum Electronics and Laser Science Conference, 2000 (QELS 2000), Technical Digest* (IEEE, 2000), p. 246.